Numerical Modelling and Resource Assessment of the NRV Geothermal Field, Colombia

Andres Jair Pinzon Mendez, John O'Sullivan, and Ken Dekkers

Department of Engineering Science, University of Auckland, 70 Symonds Street, Grafton, Auckland 1010, New Zealand

apin759@aucklanduni.ac.nz

Keywords: *Nevado del Ruiz Volcano (NRV), geothermal modelling, resource assessment, uncertainty*

ABSTRACT

The Nevado del Ruiz Volcano (NRV), located in the central cordillera of Colombia, is one of the most monitored volcanoes in the world due to its destructive capability. Thanks to this, there is abundant information regarding its surrounding structures and the behaviour of the edifice itself. This information has been used over the years to study the potential of the area to produce geothermal energy; however, because of the political and economic circumstances of the country, geothermal development has been slow and disorganised, and exploration projects have focused on understanding its geology and the geochemistry of the surface features associated with it, but the underground structures have not yet been extensively studied.

This research aimed to gather the open-source information of the field and compile it to create a geological model of the area using Leapfrog Energy 2023.1. Furthermore, this geological model was used to create a discretised numerical reservoir model, using AUTOUGH2, that matched the estimated subsurface structures and the surface manifestations found in the zone.

The calibrated numerical model of the NRV obtained matched the expected flow patterns of the field, which were estimated based on two groups of surface manifestations: group one (G1), of acidic nature, located to the west of the volcano and believed to correspond to the upflow of the field, and group two (G2), located further away from the volcano in its north-western flank, which presented alkali-chloride mixed waters and is believed to be the outflow region.

Additionally, this numerical model was used to perform a resource assessment and predict, considering uncertainty, how much power the field could produce based on a resource assessment method developed by Dekkers et al. at the University of Auckland. Using this method, the estimated NRV mean power production potential was above 150MWe over an exploitation period of 25 years, with a confidence interval P90 of about 100MWe and P10 of about 200MWe.

1. INTRODUCTION

Colombia is situated in the northeast corner of South America, and thanks to its geographical setting, it has a rich diversity of landscapes. Because of its complicated geology and extensive volcanic activity, Colombia has great potential for geothermal energy development. However, due to the political and economic circumstances of the country, the commissioning of a geothermal power plant has not yet been successful. Among the suitable locations for geothermal development, the NRV geothermal field stands as a significant potential resource and is found near an active composite volcano of the same name. The NRV is part of a series of volcanoes, located in the Ruiz-Tolima volcanic complex (RTVC) in the central cordillera of Colombia and its peak, where the Arenas crater sits, rises 5,321m.a.s.l. and is covered by a glacier with an area of 9.3 km2.

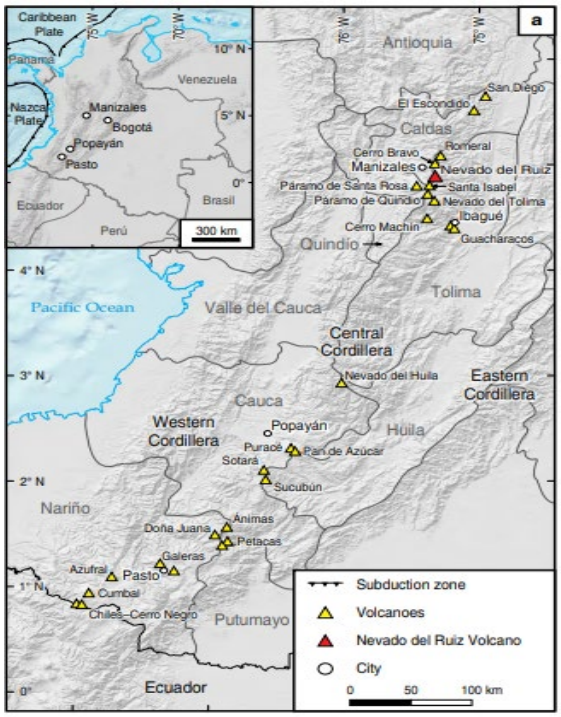


Figure 1: Localization of the NRV. Taken from The Geology of Colombia (vol.4, p. 269) by Ceballos Hernández et al., 2020.

2. METHODOLOGY

2.1 Geological model

The geological model was built using the most current field data found in various open sources and importing it into Leapfrog Energy 2023.1 as geological maps and lithological cross-sections.

2.1.1 Stratigraphy

The NRV is the largest stratovolcano of the Ruiz Tolima Volcanic Complex (RTVC) and in its vicinity, many active faults are found (Ceballos Hernández et al., 2020, p. 271). A glacial cap also covers the NRV, and the volcano itself is formed by layers of andesitic rock that have been shaped according to the period of activity. In its surrounding area, several volcanic deposits accumulated during the volcanic dome's different eruptive phases, all attributed to the quaternary period (Thouret et al., 1990, pp. 225–251). The basement of the Central Cordillera on the other hand, where the NRV is located, is mainly formed by the Cajamarca complex, which has suffered multiple metamorphisms and is composed primarily of mica-schist, phyllites and metasediments. It was shaped by a sedimentation of marine components that occurred around 240 to 220 million years

ISSN 2703-4275

ago and underwent metamorphism between 230-218 million years ago. The thickness of this unit is not currently known (González-Garcia et al., 2015, p. 2).

2.1.2 Faulting

Around the volcano, many faults are oriented in multiple directions, a consequence of the intense tectonic motion at this location. Although the interaction between the Nazca and South American plates is the leading cause of the activity, the Caribbean plate also interacts with them, and this convergence is responsible for the diversity of structural styles in the area (Cervantes, 2019, p. 12). Table 1 presents a summary of the faults included in the model and Figure 2 shows their distribution within the geological map.

Table 1: Faults and their Trend in the NRV Geothermal Field

Fault	Trend
Campoalegrito (B)	NW-SE
Olleta Nereidas (O)	NE-SW
Santa Rosa (F)	NE-SW
Pico Terrible (P)	NE-SW
Cueva Pirineos (C)	NE-SW
San Jerónimo (J)	N-S
Nereidas 1 (N)	NW-SE
Nereidas 2 (M)	NW-SE
Villamaría-Termales (V)	NW-SE
Samaná Sur 1 (S)	NE-SW
Samaná Sur 2 (T)	NE-SW
Samaná Sur 3 (U)	NE-SW
Quebrada Negra (Q)	NW-SE
Rio Claro (R)	NW-SE
Palestina (A)	NE-SW

2.1.2.1 Faults trending N-S

Although there are multiple faults that trend N-S proximal to the NRV, the only fault included in this study from this sub-set is the San Jerónimo fault, as it puts into contact the Cajamarca complex, which constitutes the core of the central cordillera, with the Quebradagrande complex to the west. This fault's orientation (along with the NW-SE group of faults) corresponds with the orientation of the Andes Mountain chain (Mejía et al., 2012, p. 30). The San Jerónimo fault is a reverse fault, and the displacement direction is leftward (Moreno et al., 2018, p. 25). In this paper, it is used as a guide to define the western boundary of the numerical model.

2.1.2.2 Faults trending NW-SE

It is a group of Normal faults located to the west of the NRV that control the watercourse of the rivers/creeks that run through them (Moreno et al., 2018, p. 31). These faults are of great importance for the study of the potential geothermal reservoir of the NRV, as there are a high number of hot springs that align with their trend (Diaz Gil & Aguirre Hoyos, 2014, p. 14).

2.1.2.3 Faults trending NE-SW

These structures are a group of strike-slip and reverse faults with a dextral component and around the area of study, they cross over the NW-SE trending faults; this interaction could have an impact on the permeability of the NRV. The Palestina fault, however, is believed to be responsible for the volcanic activity in the area, as the main volcanos of the RTVC align along the course of this fault (Moreno et al., 2018, p. 30) and in this paper is used as a guide to define the eastern boundary of the numerical model.

2.1.3 Geological Map

The geological map used as a base for the geological model and observed in Figure 2 is the one used by Cervantes M. (2019), as it has a clear representation of the lithologies of interest on the surface and the existing fractures distributed around the field.

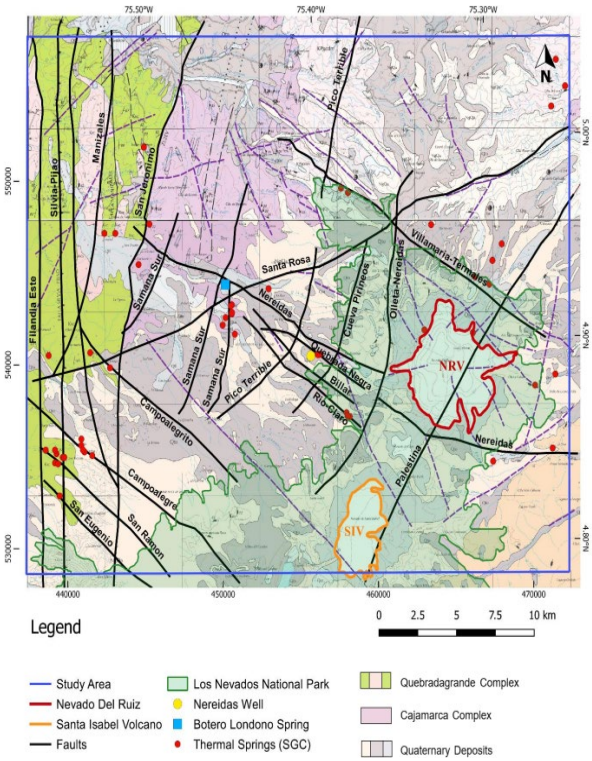


Figure 2: Geological Map of the NRV. Taken from 3D Modelling of Faulting and Intrusion of the Nevado del Ruiz Volcano, Colombia by Cervantes, p. 18, 2019

2.1.4 Geochemistry

Numerous geothermal discharges surround the NRV, which reinforces the theory that its geothermal system is fault-dominated (Lopez, 1992, p. 28). Despite this, just two groups of hot springs, found within the study area, were included in this study (Figure 3).

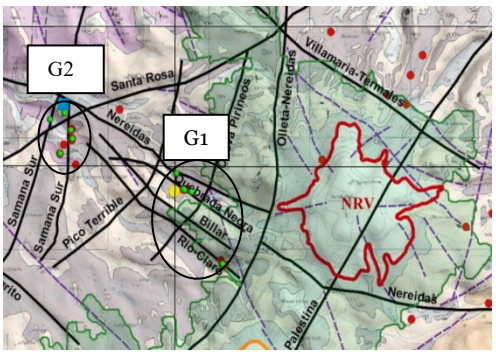


Figure 3: G1 and G2 Groups of Hot Springs Modelled as Points on Leapfrog Energy 2023.1. Adapted from 3D Modelling of Faulting and Intrusion of the Nevado del Ruiz Volcano, Colombia by Cervantes, p. 18, 2019

2.1.4.1 Group 1 (G1)

Located closer to the NRV, group 1 (G1) includes the Nereidas 1 (N1) and 2 (N2), the Nereidas well (NP) and the Chorro Negro (CN) springs. According to Taborda et al. (2022), due to their high bicarbonate and sulphate content,

ISSN 2703-4275

these surface manifestations are considered upflows of the geothermal reservoir. Compared to group 2 (G2), this cluster of thermal pools has a lesser temperature range and lower concentration of trace elements.

2.1.4.2 Group 2 (G2)

Taborda et al. also examined another group of hot springs located further down the slopes of the western flank of the volcano, group 2 (G2) of hot springs, which encompasses the Geysers (G), Quebradanegra (QN), El Bosque/La Piscina (BP) and Rio Claro (RC) hot springs. When compared with G1, G2 has a higher concentration of chloride; thus, they are closer to the water-rock equilibrium and have a higher content of trace elements, which indicates prolonged contact with the deep geothermal reservoir. Consequently, G2 is considered a possible outflow zone. Federico et al. (2017, p. 43) also studied a thermal spring (FTBL) located in this area and found that the waters were of a chloride nature, with a temperature of 79.5°C and a volume flow rate of 15L/s. For this study, this hot spring was also included in the surface manifestations as part of the G2 group.

2.1.5 Geophysics

In this paper, resistivity profiles are used to create the alteration model for the NRV. The first magnetotelluric survey carried out in the area was completed in 1993, and it included a total of 23 stations located within the area of study. However, the results of this survey were very limited for two reasons. The highly steep terrain where the potential resource is located makes it challenging to obtain and interpret the resistivity profiles of the area, and the presence of graphite in the metamorphic basement, which is believed to host the geothermal fluid, can increase the measured conductivity, giving us false signs of a high-conductivity clay cap (Almaguer Rodríguez, 2013, p. 7).

Another magnetotelluric survey by Almaguer Rodríguez (2013) consisted of 105 stations distributed over 100 km2. The severe terrain and the difficulty of access determined the location of the stations, and this had an impact on the results. 1D inversion was performed to obtain apparent resistivity maps at different depths, and the vertical resistivity profiles were produced by 2D inversion of the data. However, due to the complicated terrain and the interference of the host rock, the vertical profiles were not consistent with the presence of a clay cap and, consequently, were not included in this paper to construct the alteration model. Instead, the apparent resistivity maps at different depths, were used to estimate the alteration area.

2.1.6 Well data

The Nereidas well (as it is named due to its proximity to the Nereidas valley) was drilled in 1997, and it was the first (and only) exploratory well drilled in the western flank of the NRV (Monsalve et al., 1998, p. 263). It was initially planned to have a depth of 2,000m; however, it deviated from its course with an angle of 42°. This deviation was not intended, and extensions to the project were not considered; consequently, the final reached depth was 1,466m (Monsalve et al., 1998, p. 263). The well at this depth was not permeable; however, it was hot, with a measured bottom-hole temperature of 200°C. Nonetheless, the actual procedure to get this measurement was not specified by the researchers, and consequently, it is uncertain if the well had already warmed up when it was obtained (Cervantes, 2019, p. 42).

The geology of the well, on the other hand, provided useful information. According to Monsalve et al. (1998, p. 266), the Cajamarca complex is reached at a depth of 758.9m and the minerals found at around the 1,000m mark and below allow us to infer a reservoir temperature higher than 200°C. The presence of epidote indicates temperatures above 250°C either at present or at some time in the past (Cervantes, 2019, p. 42). Furthermore, boiling, and mineral deposition are implied to occur within the system, as adularia, calcite and silica were also found (Monsalve et al., 1998, p. 263).

2.1.7 Conceptual Model

A conceptual model for the NRV was estimated by Giggenbach et al. (1990, p. 13). This model was based solely on geochemical data and considered the system to be sealed by an impermeable carapace, which would contain the theorised two-phase reservoir. Cervantes (2019), on the other hand, proposed a conceptual model based on more recent evidence. This conceptual model can be considered an enhancement of the model proposed by Giggenbach et al., as it is in line with what they proposed, but at the same time is based on a multidisciplinary set of data, which was obtained over the 30 years since the first conceptual model was suggested.

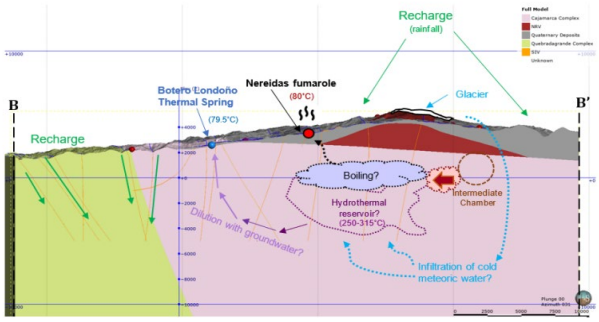


Figure 4: NRV Conceptual Model. Taken from 3D Modelling of Faulting and Intrusion of the Nevado del Ruiz Volcano, Colombia by Cervantes, p. 82, 2019

2.1.8 Geological Model Creation

The data collected in the literature review served as the base for constructing the 3D geological model of the NRV by using Leapfrog Energy 2023.1.

The primary source on which the lithological units were based was the geological map from Cervantes M. (2019) (Figure 2). A cross-section from Vélez et al. (2018, p. 157) was also used to define the contacts between the main lithologies, and a cross-section from Ceballos Hernández et al. (2020, p. 281) was used to estimate the underground boundaries of the volcano (Figure 5). The topography of the area defined the upper boundary of the geological model, and the lower boundary was set at -1,000m.a.s.l. The surface on the other hand was modelled according to the geological map; however, the upper lithologies are not considered to have a significant influence on the resource (Monsalve et al., 1998, p. 263), and therefore, in this paper, are group together as a single lithological unit. The final geological model of the area can be observed in Figure 6.

2.1.9 Alteration Model Creation

Although important for our purposes, the clay cap for the NRV geothermal field, theoretically, would have less control over the system, as the host rock itself is considered to have

ISSN 2703-4275

a low permeability due to its metamorphic nature, and consequently, the system is expected to be fault-dominated. Nevertheless, clay alteration minerals were found within the structures of the Nereidas well and are deemed to have an impact on the system (Cervantes, 2019, p. 43).

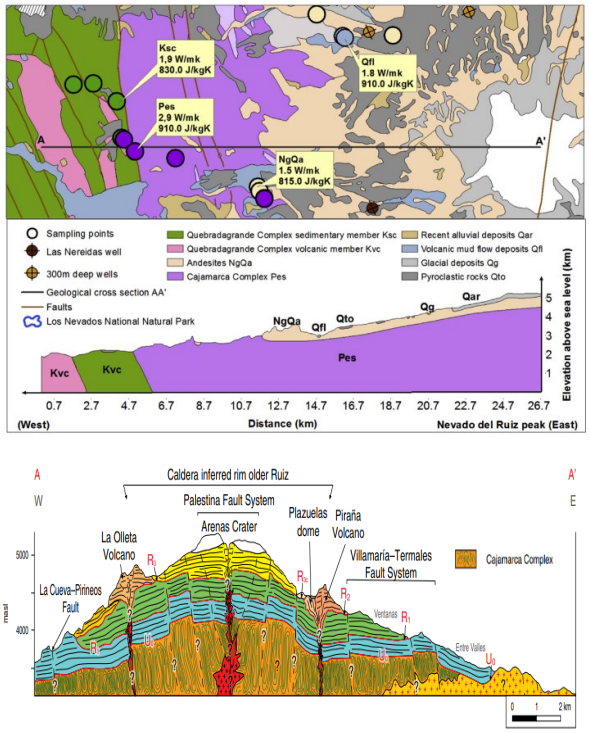


Figure 5: Geological Cross-section W-E of the NRV from Vélez et al. (Above), Cross-section W-E of the NRV Volcanic Cone from Ceballos Hernández et al. (Below)

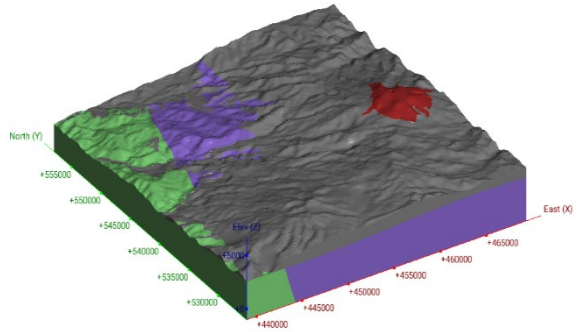


Figure 6: 3D Geological Model of the NRV

The primary dataset utilised to model the clay cap was the apparent resistivity maps at different depths obtained by Almaguer Rodríguez (2013). The apparent maps were imported into Leapfrog Energy 2023.1 by using the topography as a reference and creating meshes with it at different depths, then associating each mesh to the respective apparent resistivity map (Figure 7). Following this, the MT profiles from Trujillo Vargas (2022) and González-Garcia et al. (2015) were used to improve its shape (Figure 8). After obtaining an alteration model based on this data set, this was reinterpreted to reduce the inconsistencies.

2.1.10 Structural Model Creation

The structural model includes several proven faults around the area of study, and this is critical for the NRV geothermal field, as the system is believed to be dominated by the secondary permeability produced by the fractures, and not by the permeability of the host rock (Lopez, 1992, p. 28). Fifteen faults were modelled on Leapfrog Energy 2023.1 and their dipping angle was decided using different sources. Faults S, C, N, M, Q, R, P and V were modelled after Cervantes' (2019) suggestions and all the other faults were modelled by using cross-sections from several authors (Vélez et al., 2018, p. 157), (Moreno et al., 2018, p. 58), (Ceballos Hernández et al., 2020, p. 281), (Taborda et al., 2022, p. 4). The final structural model is presented in Figure 9.

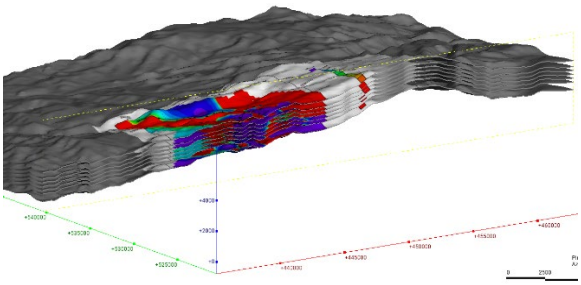


Figure 7: Topography Meshes with Apparent Resistivity Maps at Different depths

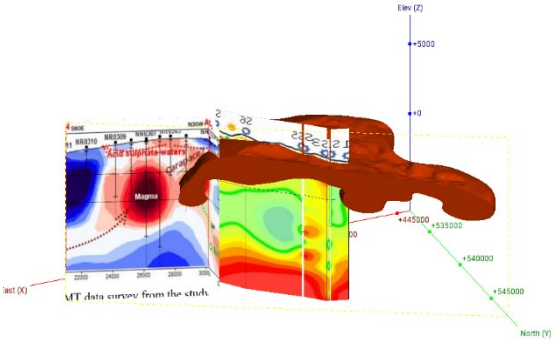


Figure 8: Vertical Profiles Used to Improve the Modelling of the Clay Cap

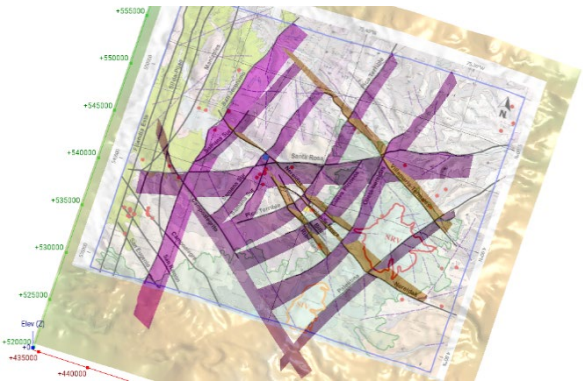


Figure 9: Structural Model of the NRV

2.1.11 Numerical Model Creation

The accuracy of the numerical model for a particular geothermal field will depend on the precision of the scientific data available, which, in the case of the NRV, is very limited. The only existing exploratory well was hot but not permeable since the target was probably missed (García Jiménez et al., 2013, p. 946), and the method in which the 200°C bottom-hole temperature was measured is not mentioned in the literature; hence, this value could be underestimated (Cervantes, 2019, p. 42). Furthermore, as there are no wells that have been drilled deep enough into the Cajamarca complex, host rock properties, such as density, permeability,

ISSN 2703-4275

porosity, and thermal conductivity, cannot be measured at the reservoir level, which decreases the accuracy of the model (Franco & Vaccaro, 2014, p. 988). Nonetheless, Oviedo et al. (2023, p. 9) measured rock properties from outcrops of exposures of the Cajamarca complex at different locations across the greenfield and obtained values of porosity, permeability, and thermal conductivity, which served as an approximation to the properties of the host rock in the numerical model.

The model extension was defined by four faults considered to enclose the resource as an approximation to the limits for the boundary condition (faults J, V, B and A). The model orientation, on the other hand, follows the pattern of the NW-SE trending faults, believed to have an important control over the system (N, Q and R) since it is assumed that the resource is potentially contained below this area. Additionally, the size of the resistivity anomaly was also considered when defining the proportions of the model, setting a limit of about 5 km beyond the extension of the clay cap to capture the meteoric recharge of the system. The model has a rectangular extent of 22km along the centred NW-SE trending faults and 16km in the direction perpendicular to them. It is composed of 32,358 blocks with varying resolutions depending on the location of the blocks. The centre of the field (covering the N, Q and R faults), where the resource is believed to be contained, has a horizontal resolution of 500 m x 500 m per block, while the surrounding sections have a resolution of 1000 m x 1000 m per block. The vertical resolution varies from the top to the bottom to create a more accurate representation of the field, where geological elements can have a higher variability of properties based on their interaction with each other. The resolution is highest at the top with 50m per block and lowest at the bottom with 500m per block, with intermediate values of 100m and 200m.

2.1.11.1 Boundary Condition

First, the top boundary of the model was defined by the blocks that compose the top surface of the field and the properties assigned to them. Dry conditions were simulated, with an approximated pressure of 1 bar across the field and temperature varying with height to make it consistent with the severe topography of the terrain. The average precipitations of 2,000 -2,500 mm p.a. (Colparques, n.d.) and the glacial cover that extends 25km2 over the volcano and suffers constant melting processes (Pierson et al., 1990, p. 20), were also considered when assigning the boundary conditions to the top blocks of the model. Secondly, and as suggested by O'Sullivan et al. (2000, p. 4066), no flow boundary conditions were used for this model, which is in accordance with the expected flow distribution based on the idea that the faults act as barriers and enclose the system. Finally, the bottom boundary of the model that defines the heat and mass input at the base of the reservoir was distributed along the SW-NE trending faults closest to the volcano (O and C), with higher generation values at their intersection with the NW-SE trending faults believed to control the flow (N, Q and R) (Figure 10). The background heat flux instead, was defined as 80mW/m2. It is important to note that the distribution and strength of the deep upflow boundary condition were determined as part of the calibration process.

2.1.11.2 Rock Properties

The properties assigned to the rocks vary across the field depending on the discretisation process used to create the numerical model. This process classifies each block based on the lithology it is made of, the location in the reservoir, and the structures that cross over it. For the NRV, the combination of interactions produced 304 rock types.

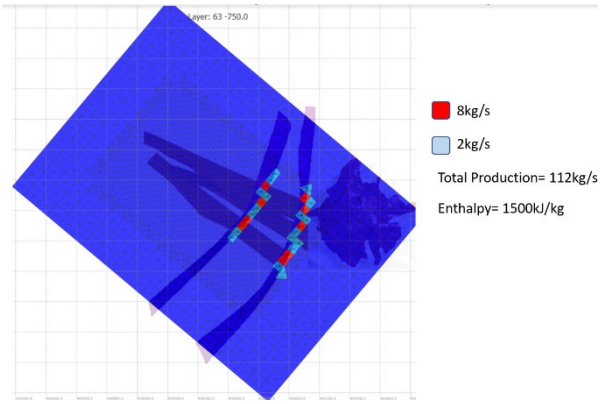


Figure 10: Bottom Boundary of the NRV Geothermal Field Numerical Model

For this field in particular, the presence of multiple lithological units was not a defining factor when creating the numerical model, as the evidence suggests that the Cajamarca complex contains the resource and is, therefore, the only lithology believed to have an impact on it. Nonetheless, within the area of study, and with the boundaries selected, it is a thick unit, and therefore, the bottom layers of the model are likely to have lower permeability values when compared to the upper layers, hence, they were assumed to be a different lithological unit. Table 2 shows the nomenclature used to classify the different rock types.

Table 2: Structures and lithologies of the Numerical Model of the NRV

Geologic unit		Faults	
K	Quebradagrande Complex	San Jerónimo	J
Q	Quaternary Deposits	Samaná Sur 1	S
P	Cajamarca Complex	Samaná Sur 2	T
B	Deep Cajamarca Complex	Samaná Sur 3	U
N	Nevado del Ruiz Volcano	Pico Terrible	P
		Cueva Pirineos	C
Alteration		Olleta-Nereidas	O
A	Present	Nereidas 1	N
0	Absent	Nereidas 2	M
		Quebradanegra	Q
		Rio Claro	R
		Santa Rosa	F
		Villamaría-T	V
		Palestina	A

2.1.11.3 Natural State Model

To obtain a numerical model that represents the current data of the unexplored field (natural state), an initial model was set up with typical properties for the different rock types and estimated deep upflow boundary conditions, defined at the bottom layer of the model, and it was followed by a calibration process that consisted of varying permeabilities of the rock types and heat and mass upflow strength and distribution at the bottom layer. The generation blocks were assigned with a higher strength to the intersections of the C and O faults with the N, Q and R faults, as they are assumed to be the areas with more fractures and, accordingly, a better conduit for the resource, with additional generation blocks

ISSN 2703-4275

along the C and O faults to improve the flow, but always maintaining a higher production rate at the intersections.

For the NRV numerical model, initial calibration was defined as satisfactory when the heat flow pattern followed the shape of the interpreted alteration zone, with temperatures of at least 200°C below the clay cap. This was the measured downhole temperature of the Nereidas well and therefore the only approximation to the alteration zone temperatures (Cervantes, 2019, p. 42). Nevertheless, this was not achieved uniformly due to the lack of faults that could increase the flow in certain areas, especially in the more distal zone from the NRV, around the location of the estimated outflow. Still, as there is a high level of uncertainty, calibration was deemed concluded by considering the flow pattern and when the heat flow followed the shape of the clay cap (Figure 11).

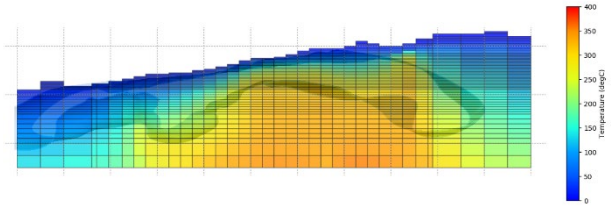


Figure 11: Cross-section of the NRV Numerical Model, Parallel to the NW-SE Trending Faults (N, Q and R), Estimated to Control the Flow of the Resource

2.1.10 Resource Assessment

With the high level of investment and, consequently, the risk that geothermal projects represent, it is disconcerting how power generation estimates are still based on rough measurements of the rock properties, and on highly uncertain assumptions about the shape and extension of the geothermal field. Vélez et al. (2018, pp. 161–163) performed a resource assessment to estimate the potential power generation capacity of the NRV geothermal field using the traditional method, which is based on inferred rock properties of the deep geothermal reservoir. These properties were determined by studying several samples from outcrops of the Cajamarca complex at different locations, as well as a 2D simulated temperature model obtained with the software OpenGeoSys, which utilised an inferred geological cross-section. They determined the geothermal generation potential to be within the range of 30-40Mwe, however, as described before, the assumptions made to determine this value make this estimate highly unreliable.

Before beginning the resource estimation process, additional upflow blocks were added to the bottom layer of the field to improve the flow towards the North-West area, where the outflow is located, enhancing the likelihood of convergence. This adjustment was made based on the assumption that the heat source is found at a deeper level than the bottom boundary condition, and therefore the NE-SW trending fault P could also be a pathway for the geothermal fluid and, consequently, another upflow region. The generation rate at this fault, however, was kept at lower levels when compared to C and O to maintain consistency with the initial numerical model.

Dekkers, Gravatt, Maclaren, et al. (2022) method uses the natural state calibrated model to generate multiple sample models with variable permeabilities and alternative upflow distributions. For the case of the NRV, 1000 models were generated and then run to steady-state conditions using the Waiwera geothermal simulator. A time limit of 15 min was established to make them converge to natural state, and the ones that converged, 690 in this case, were included in the set of possible scenarios.

The selected models were then subjected to a two-step conditioning process. First, and more highly weighted, was the conditioning of the alteration zone, which was performed with an assumed temperature of 190°C for the blocks directly below the clay cap and closest to the surface, typically located in the inner zones of the alteration. A second conditioning, with a lesser weight, was carried out by matching the blocks on the surface where thermal manifestations were found; This was done based on the temperature of the corresponding hot springs and the flow rate for hot spring FTBL, the only one with a reported value in the literature. This process was completed using the Approximate Bayesian Computation (ABC) method. The blocks in the deeper zones of the alteration were not considered for conditioning because there is higher uncertainty of the MT data at depth (Dekkers, Gravatt, Maclaren, et al., 2022, pp. 2–4). The conditioning process yielded 200 filtered sample models. Figure 12 shows an example of included and excluded models.

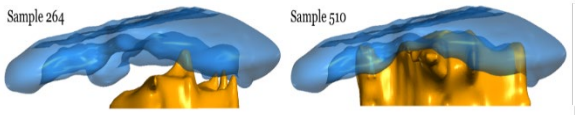


Figure 12: Example of Rejected (left) and Included (right) Models for the Resource Assessment of the NRV.

Finally, production scenarios were run for every selected model by targeting the blocks with the best flow conditions as potential wells and running the production model for 25 years, repeating the run with each new additional well. Block targets for reinjection wells were selected based on the pressure drop they would experience after the set production time, with highest pressure drop being a criterion for possible reinjection locations. Every natural state model was run iteratively until reaching a less than 5% increase in steam flow rate compared with the previous run for production, and a sensible pressure drop limit for reinjection. This process was repeated for every model, generating a distribution of power output forecasts. The models were run in parallel, and each run took approximately 5 minutes.

3. RESULTS

3.1 Numerical Model

The final numerical model of the NRV geothermal system was obtained after calibration when the flow pattern matched the shape of the clay cap. After finalising the model, however, consistency with surface manifestation was checked, observing how they correspond with the acidic surface features (G1) and alkali-chloride surface features (G2). To analyse how the geothermal system behaves, a vertical cross-section of the numerical model, parallel to the NW-SE trending faults that control the flow (N, Q and R) and crossing over the surface manifestations was obtained. Figure 13 shows how the geothermal fluid behaves below the surface, with recharge coming from rain and the melting of the glacial cap that infiltrates the upper rock layers, which are primarily volcanic deposits and, therefore, have relatively high permeability (Oviedo et al., 2023, p. 9).

ISSN 2703-4275

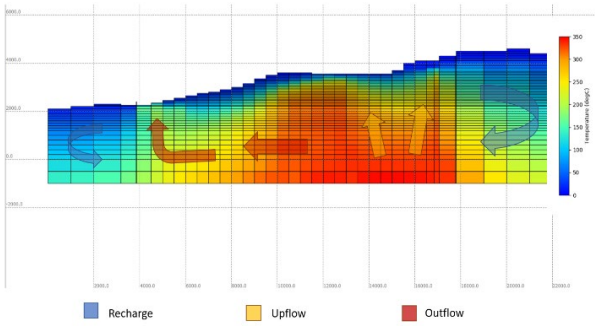


Figure 13: Cross-section of the NRV Numerical Model. Arrows Represent the Flow Patterns

A Leapfrog Energy 2023.1 visualisation of the numerical model was generated by importing the temperature data from the calibrated natural state model (Figure 14). As we can observe in this model, the meteoric and glacial waters infiltrate the system via permeable rocks at the surface and permeable fractures at depth. In addition, multiple faults can potentially play a part in the recharge of the system. The generating deep boundary condition, placed across the strike of the O and C faults at the bottom layer of the numerical model, is observed in Figure 14 as the point of origin of the heat flow, which travels upwards through the pathways created by these faults. An impermeable (clay cap) zone, in accordance with the conceptual model from Cervantes (2019, p. 81), blocks the geothermal liquid fluid from continuing to travel upwards. However, the gases and steam reach the surface, generating acidic surface manifestations belonging to the G1 hot springs cluster, considered the upflow of the system (Taborda et al., 2022, p. 10). This further agrees with Cervantes's (2019, p. 81) theorised presence of boiling. The geothermal fluid then travels across the field via the central NW-SE trending faults that are not observed in the cross-section, as it is parallel to them, finally reaching the surface at the location of the G2 cluster of thermal springs, which are believed to be the outflow of the system (Taborda et al., 2022, p. 10). As previously studied by Moreno et al. (2018, pp. 60–61), and according to the created model, the faults that seem to be responsible for the outflow zone are the group of the Samaná fault system because it is via these conduits that the geothermal fluid seems to travel upwards, to end up surfacing as alkali-chloride mixed waters.

3.2 Resource Assessment

Production predictions for 25 years were run for the selected 200 models, obtaining a distribution of parameters over a set time interval. Figure 15 shows how, according to the current field data utilised to obtain the numerical model, there is a mean estimated resource potential of about 150MWe power output, with a confidence interval P90 at above 100MWe and P10 at above 200MWe over a period of 25 years.

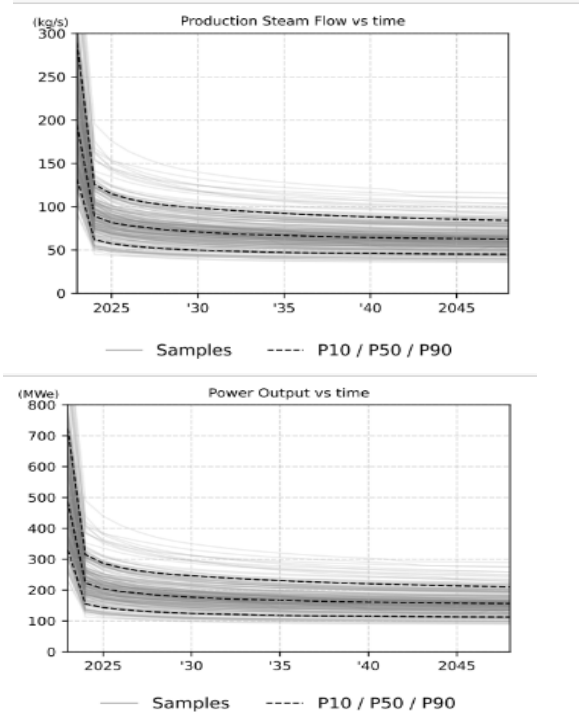


Figure 15: Distribution of the Estimation of Steam Flow Production (Above) and Power Output (Below) for the NRV.

4. DISCUSSION

The numerical model of the NRV greenfield facilitated the understanding of the flow processes within the Cajamarca complex, the host rock of the geothermal fluid. Furthermore, the final calibrated model was used to estimate the potential for energy generation of the field, based on more accurate

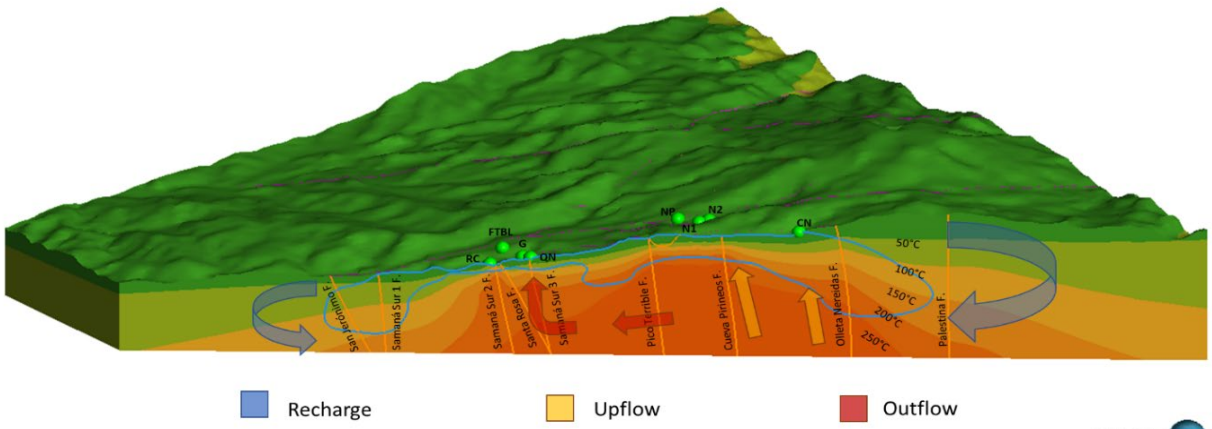


Figure 14: Conceptual Model of the Leapfrog Energy 2023.1 Numeric Model Based on Natural State Model Temperature Data of the NRV Geothermal Field

ISSN 2703-4275

methods than the simple calculations sometimes utilised for projects of this magnitude. The metamorphic host rock has an intrinsic low permeability (Oviedo et al., 2023, p. 9), and the NRV geothermal field is characterised by the high amount of secondary permeability due to the fractures that populate the area (Cervantes, 2019, p. 12). However, as mentioned by Aguilera and Adam (2020, pp. 4–5) the anisotropic elasticity of this formation could be vital to understanding how this basement, which extends across the central cordillera of the country, can host a geothermal reservoir. The secondary permeability, however, can still be regarded as the main driving factor that controls the system.

Some assumptions were made to obtain a model that closely represented the field. First, the resource was assumed to be contained within the J, V, A and B. This approximation seems accurate for J, a reverse fault that acts as a suture of two different lithologies (Mejía et al., 2012, p. 31), and it likely acts as a barrier. It is also applicable to faults V and A, which are structures that, according to the literature, are thought to control the volcanism of the area. However, fault B is a normal fault with surface manifestations located near the area where it crosses J, and despite these springs being too distant from the volcanic heat source, there is no evidence to assume that they are not connected to the NRV geothermal reservoir (Cervantes, 2019, p. 23). Furthermore, the uncertainty of the MT data, due to the severity of the terrain and the interfering graphite content of the host rock made the modelling process challenging because the reliability of the modelled alteration zone is mainly based on highly uncertain resistivity profiles, and interpretation of its shape was necessary to obtain a usable model. Despite the limitations, however, the natural state flow pattern was consistent with the estimated upflow and outflow zones and with the modelled shape of the clay cap. This allowed us to use the calibrated numerical model as an approximate representation of the fluid movements within the reservoir.

During the resource assessment process, a high number of possible scenarios, based on the initial calibrated model, were created. This process ultimately takes into consideration the uncertainty associated with the data and accounts for it by assuming a high number of equally likely possibilities. The conditioning process, on the other hand, reduces the number of possibilities by filtering the results according to reasonable assumptions, which fine-tune the calibrated natural state model, matching parameters that were challenging to satisfy during the manual refinement process performed while calibrating the numerical model.

The mean estimation of power output obtained was above 150MWe for the NRV, considerably higher than the one obtained by Vélez et al. (2018, p. 163), which was within the range of 30-40MWe. This illustrates the importance of more careful geothermal resource estimations that include a range of data from different disciplines and provide a more accurate prediction that allows for more informed decision-making in projects with such high risk involved. The set of models utilised for the analysis was chosen after careful screening, selecting the optimal models based on different statistical methods. However, the outcome is based on all the assumptions made during the development of the model. Consequently, including the interval of confidence P90 and P10 takes the uncertainty inherent to the process into account. With the P90 value, we can observe that even the more conservative estimation provides a prediction for power output of above 100MWe, which still sits well above the estimation made by Vélez et al.

Finally, it is essential to note that the quality of the results will always depend on the quality of the input data and, hence, the exploration phase of the greenfield is critical. A multidisciplinary approach to understanding the subsurface structures is vital to obtaining a resource estimate that will ultimately mitigate the risk of a highly uncertain endeavour.

5. CONCLUSION

To produce an accurate estimate of the power production potential of any geothermal field, the quantity and quality of the field data is of great importance, and in our case, this data was extensive in some areas, but lacking in others, which presented challenges and difficulties to create and calibrate the numerical model. Despite this, a numerical model that matched the modelled structures was obtained, serving as input for the resource assessment of the NRV.

If we are conservative, the NRV geothermal field could produce at least 100MWe based on the P90 confidence interval, and this value is considerably higher than previous reported estimations. However, it is still considered uncertain as the data available was limited and human interpretation played a key role when developing the models. Nevertheless, previous estimations were performed based on more random assumptions, which are very common in the exploration phases of a geothermal project, and therefore, the result of this research can be considered a more precise estimation.

The present study's aim to contribute to the understanding of the subsurface processes that occur below the NRV geothermal field, was ultimately achieved, as the numerical model matches previous conceptual models, nonetheless, time constraints and the inability to access more complete industry data, conditioned the nature of the results obtained. Additionally, the resource assessment also relies heavily on the resistivity accurately identifying the size of the clay cap, hence, exploration wells should be drilled to confirm or deny the location and extent of the interpreted alteration zone. Ultimately, a numerical model is an important tool in geothermal exploration, development and exploitation, and models are never an exact representation of the fields and are constantly evolving and improving their quality as more information is obtained. Thus, this paper can be considered only as an initial step in developing the numerical model of the NRV, and accordingly in understanding the system and how it can be successfully exploited.

ACKNOWLEDGEMENTS

The authors would like to acknowledge the assistance of Seequent for their provisions of research license for Leapfrog Energy 2023.1, and the use of New Zealand eScience Infrastructure (NeSI) high performance computing facilities as part of this research.

REFERENCES

Aguilera, P. & Adam, L. (2020). Anisotropic Geothermal Host Rock? Case Study of Nevado del Ruiz, Colombia. 42nd New Zealand Geothermal Workshop.

Almaguer Rodríguez, J. de L. (2013). Estudio Magnetotelúrico con fines de interés geotérmico en el

sector norte del Nevado del Ruiz, Colombia. Universidad Nacional Autónoma de México.

Ceballos Hernández, J. A., Martínez Tabares, L. M., Valencia Ramírez, L. G., Pulgarín Alzate, B. A., Correa Tamayo, A. M. & Narváez Marulanda, B. L. 2020. (2020). Geological Evolution of the Nevado del Ruiz Volcanic Complex. (J. Gómez & A. O. Pinilla Pachon (eds.); Vol. 4, pp. 267–296). Servicio Geológico Colombiano. https://doi.org/10.32685/pub.esp.38.2019.07

Cervantes, C. A. M. (2019). 3D Modelling of Faulting and Intrusion of the Nevado del Ruiz Volcano, Colombia Thesis of 60 ECTS credits Master of Science (M.Sc.) in Sustainable Energy. Reykjavik University.

Colparques. (n.d.). Los Nevados, Parque Nacional Natural. Organización Colparques. Retrieved October 26, 2023, from http://www.colparques.net/NEVADOS

Dekkers, K., Gravatt, M., Maclaren, O. J., Nicholson, R., Nugraha, R., O'Sullivan, M., Popineau, J., Riffault, J. & O'Sullivan, J. (2022, February). Resource Assessment: Estimating the Potential of a Geothermal Reservoir. 47th Workshop on Geothermal Reservoir Engineering.

Dekkers, K., Gravatt, M., Renaud, T., Maclaren, O. J., Nicholson, R., O'Sullivan, M., Riffault, J. & O'Sullivan, J. (2022, November). Resource Assessment: Estimating the Potential of an African Rift Geothermal Reservoir . 9th African Rift Geothermal Conference

Diaz Gil, A. & Aguirre Hoyos, L. M. (2014). Análisis Estructural Detallado de un Sector del Valle de Nereidas, Macizo Volcánico Nevado del Ruiz, MVNR. Aporte al Proyecto Geotérmico EPM-CHEC. Universidad de Caldas.

Federico, C., Inguaggiato, S., Chacón, Z., Londoño, J. M., Gil, E. & Alzate, D. (2017). Vapour discharges on Nevado del Ruiz during the recent activity: Clues on the composition of the deep hydrothermal system and its effects on thermal springs. 346, 40–53. https://doi.org/10.1016/j.jvolgeores.2017.04.007

Franco, A. & Vaccaro, M. (2014). Numerical simulation of geothermal reservoirs for the sustainable design of energy plants: A review. 30, 987–1002. https://doi.org/10.1016/j.rser.2013.11.041

García Jiménez, R. D., Gutiérrez Yermanos, L., Pareja Pérez, E. R., Pusquin Ospina, L. T., Dewhurst, W. T. & López, J. P. (2013). Case Study and First Look: Contemporary Magnetotelluric Studies Within Nereidas Valley, Nevado Del Ruiz Volcano, Colombia. 37.

Giggenbach, W. F., Garcia P., N., Londoño C., A., Rodriguez V., L., Rojas G., N. & Calvache V., M. L. (1990). The chemistry of fumarolic vapor and thermal-spring discharges from the Nevado del Ruiz volcanic-magmatic-hydrothermal system, Colombia (Vol. 42, Issues 1–2, p. 13). Elsevier BV. https://doi.org/10.1016/0377-0273(90)90067-p

González-Garcia, J., Hauser, J., Annetts, D., Franco, J., Vallejo, E. & Regenauer-Lieb, K. (2015). Nevado Del Ruiz Volcano (Colombia): A 3D Model Combining Geological and Geophysical Information.

Lopez, D. (1992). The Hydrothermal System of Nevado Del Ruiz Volcano, Colombia. Louisiana State University Libraries. https://doi.org/10.31390/gradschool_disstheses.5331

Mejía, E. L., Francisco Velandia, ;, Zuluaga, C. A., López, J. A. & Cramer, T. (2012). Análisis Estructural al Noreste del Volcán Nevado del Ruiz, Colombia - Aporte a la Exploración Geotérmica. 34. https://doi.org/10.2307/j.ctvc5pc42.15

Monsalve, M. L., Rodriguez, G. I., Mendez, R. A. & Bernal, N. F. (1998). Geology of the Well Nereidas 1, Nevado Del Ruiz Volcano, Colombia. 22.

Moreno, D., Lopez-Sanchez, J., Blessent, D. & Raymond, J. (2018). Fault characterization and heat-transfer modeling to the Northwest of Nevado del Ruiz Volcano. 88, 50–63. https://doi.org/10.1016/j.jsames.2018.08.008

O'Sullivan, M. J., Pruess, K. & Lippmann, M. J. (2000). Geothermal Reservoir Simulation: The State-of-Practice and Emerging Trends. 4065–4070.

Oviedo, M. J., Blessent, D., López-Sánchez, J. & Raymond, J. (2023). Contribution to the characterization of the Nevado del Ruiz geothermal conceptual model based on rock properties dataset. 124, 104259. https://doi.org/10.1016/j.jsames.2023.104259

Pierson, T. C., Janda, R. J., Thouret, J.-C. & Borrero, C. A. (1990). Perturbation and melting of snow and ice by the 13 November 1985 eruption of Nevado del Ruiz, Colombia, and consequent mobilization, flow and deposition of lahars (Vol. 41, Issues 1–4, p. 17). Elsevier BV. https://doi.org/10.1016/0377-0273(90)90082-q

Taborda, A., Portela, J. P., Lopez-Sanchez, J., Daniele, L., Moreno, D. & Blessent, D. (2022). Temperature estimation of the Nevado del Ruiz Volcano geothermal reservoir: Insight from western hot springs hydrogeochemistry. 240, 107049. https://doi.org/10.1016/j.gexplo.2022.107049

Thouret, J.-C., Cantagrel, J. M., Salinas, R. & Murcia, A. (1990). Quaternary eruptive history of Nevado del Ruiz (Colombia). 41(1), 225–251. https://doi.org/10.1016/0377-0273(90)90090-3

Trujillo Vargas, J. S. (2022). Imaging of the Heated Subsurface Structures Beneath the Western Flank of Nevado del Ruiz Volcano, Colombia. Universidad Nacional de Colombia.

Vélez, M. I., Blessent, D., Córdoba, S., López-Sánchez, J., Raymond, J. & Parra-Palacio, E. (2018). Geothermal potential assessment of the Nevado del Ruiz volcano based on rock thermal conductivity measurements and numerical modeling of heat transfer. 81, 153–164. https://doi.org/10.1016/j.jsames.2017.11.011